Chem. Mater. **1996,** *8,* 2542−2544

Morphological Origin of High Mobility in Pentacene Thin-Film Transistors

Joyce G. Laquindanum, Howard E. Katz,*
Andrew J. Lovinger,* and Ananth Dodabalapur

Bell Laboratories, Lucent Technologies
600 Mountain Ave.
Murray Hill, New Jersey 07974

Received July 11, 1996

Organic materials have received considerable attention as active semiconductors for device applications such as Schottky diodes[1] and thin-film transistors (TFTs).[2] Two of the earliest p-type organic semiconducting materials investigated for TFT purposes were an oligothiophene, α-hexathienylene (α-6T), and pentacene. Earlier works by Garnier and co-workers have reported field-effect mobilities (μ_{FET}) of 5×10^{-4} for α-6T and 2×10^{-3} cm^2 V^{-1} s^{-1} for pentacene.[3] However, of these two materials, more exhaustive studies have been done on α-6T over pentacene. For example, it was shown by Katz and co-workers that by careful synthesis and purification of α-6T, mobilities above 0.01 cm^2 V^{-1} s^{-1} and on/off current ratios of up to 10^7 can be achieved.[4] Garnier obtained μ_{FET} of 2.5×10^{-2} by depositing the α-6T at elevated substrate temperatures.[5] α-6T TFTs have also been the subject of numerous physical characterization and device studies. [6]

Pentacene TFTs, however, have received much less attention. A TFT using a pentacene precursor processed from solution and thermally converted to pentacene with the highest field effect mobility of 9×10^{-3} cm^2 V^{-1} s^{-1} was reported.[7] Pentacene TFTs were also prepared by molecular beam deposition which yielded mobilities of up to 0.03 cm^2 V^{-1} s^{-1}.[8] More recently, mobilities as high as 0.6 cm^2 V^{-1} s^{-1} were reported for pentacene TFTs using top-contact electrode geometries by Jackson and co-workers.[9] In this communication, we report a simultaneous morphological and electrical characterization of pentacene TFT films. We obtain mobilities nearly as high as recently reported[9] and propose that the high mobility is associated with the macroscopic single-crystal nature of sublimed pentacene films.[10]

Experimental Section

Pentacene was purchased from Aldrich Chemical Co. and was purified using vacuum sublimation at 10^{-4} Torr or lower. TFTs with channel lengths $L = 1.5$, 4, 12, and 25 μm and channel width $W = 250$ μm were fabricated on thermally oxidized Si substrates as previously described.[11] The Si, with a gold ohmic contact, functions as the gate, and the oxide (thickness = 300 nm) as the gate dielectric. Pentacene was vacuum deposited (rate = 5 Å/s) on top of the contacts at pressures of 2×10^{-6} Torr to form films ca. 500 Å thick. In this experiment, three different substrate temperatures (T_{sub}) were used during deposition by heating the copper block on which the substrates were mounted. TFT characterization was done at room temperature under vacuum using a Hewlett-Packard 4145B semiconductor parameter analyzer at varying gate voltages.

For morphological studies, pentacene was vacuum evaporated onto Si/SiO$_2$ and carbon-coated electron-microscope grids simultaneously with the TFTs. The deposited films were about 500 Å thick; those used for electron microscopy were subsequently shadowed with Pt/C at $\tan^{-1} {}^{1}/_{2}$ (to increase contrast) and lightly carbon-coated in a vacuum evaporator prior to examination in a JEOL transmission electron microscope at 100 kV. Pentacene films on Si/SiO$_2$ were used for X-ray diffraction studies in the reflection mode at 40 kV and 25 mA with scanning rates of 1.0° 2θ/min and Ni-filtered CuKα radiation from a 2-kW Rigaku X-ray generator.

Results and Discussion

The drain-source current−voltage (I_{DS}−V_{DS}) characteristics were measured for pentacene films deposited at different substrate temperatures. Figure 1a,b shows the I−V characteristics of a 12-μm channel length device for $T_{\mathrm{sub}} = 25$ and 85 °C, respectively. The mobilities were measured in the saturation regime ($V_{\mathrm{DS}} > V_{\mathrm{GS}}$), which is modeled by the equation[12]

$$I_{\mathrm{DS}} = \frac{WC_{\mathrm{i}}}{2L}\mu(V_{\mathrm{G}} - V_0)^2 \tag{1}$$

where μ is the field-effect mobility, L and W are channel length and width, respectively, C_{i} is the insulator capacitance per unit area (for 300 nm SiO$_2$, C_{i} is 10 nF/cm^2), and V_0 is the extrapolated threshold voltage. The latter is the voltage at which the conduction channel begins to form and can be extracted from the plot $I_{\mathrm{DS}}{}^{1/2}$ vs V_{G} (Figure 1a and b inset). By extrapolating to the V_{G} axis, V_0 of −15 V for $T_{\mathrm{sub}} = 25$ °C and −22 V for $T_{\mathrm{sub}} = 85$ °C were calculated. Thus, for the plots on Figure 1a,b, μ of 0.16 and 0.4 cm^2 V^{-1} s^{-1} were calculated. These mobilities are similar to the hole mobilities measured at room temperature in highly purified single crystals of naphthalene and anthracene by transient photoconductivity techniques.[13] On/off ratios, i.e., between I_{DS} currents at $V_{\mathrm{G}} = -100$ V and $V_{\mathrm{G}} = 0$

---

(1) (a) Fichou, D.; Horowitz, G.; Nishikatani, Y.; Roncali, J.; Garnier, F. *Synth. Met.* **1989**, *28*, C729. (b) de Leeuw, D. M.; Lous, E. J. *Synth. Met.* **1994**, *65*, 45.

(2) (a) Horowitz, G.; Fichou, D.; Peng, X.; Garnier, F. *Solid State Commun.* **1989**, *72*, 381. (b) Tsumura, A.; Koezuka, H.; Ando, K. *Appl. Phys. Lett.* **1986**, *49*, 1210. (c) Assadi, A.; Svensson, C.; Willander, M.; Ingannas, O. *Appl. Phys. Lett.* **1988**, *53*, 195. (d) Fuchigami, H.; Tsumura, A.; Koezuka, H. *Appl. Phys. Lett.* **1993**, *63*, 1372. (e) Paloheimo, J.; Kuivalainen, P.; Stubb, H.; Vuorimaa, E.; Yli-Lahti, P. *Appl. Phys. Lett.* **1990**, *56*, 1157.

(3) Horowitz, G.; Fichou, D.; Peng, X.; Garnier, F. *Synth. Met.* **1991**, *41−43*, 1127.

(4) Katz, H. E.; Torsi, L.; Dodabalapur, A. *Chem. Mater.* **1995**, *7*, 2235.

(5) Servet, B.; Horowitz, G.; Ries, S.; Lagorsse, O.; Alnot, P.; Deloffre, F.; Srivastava, P.; Hajlaoui, R.; Lang, P.; Garnier, F. *Chem. Mater.* **1994**, *6*, 1809.

(6) (a) Garnier, F.; Peng, F. Z.; Horowitz, G.; Fichou, D. *Adv. Mater.* **1990**, *2*, 592. (b) Peng, X.; Horowitz, G.; Fichou, D.; Garnier, F. *Appl. Phys. Lett.* **1990**, *57*, 2013. (c) Dodabalapur, A.; Katz, H. E.; Torsi, L.; Haddon, R. C. *Science* **1995**, *269*, 1560. (d) Torsi, L.; Dodabalapur, A.; Katz, H. E. *J. Appl. Phys.* **1995**, *78*, 1088. (e) Torsi, L.; Dodabalapur, A.; Rothberg, L. J.; Fung, A. W. P.; Katz, H. E. *Science* **1996**, *272*, 1462.

(7) (a) Brown, A. R.; Pomp, A.; de Leeuw, D. M.; Klaasen, D. B. M.; Havinga, E. E.; Herwig, P.; Mullen, K. *J. Appl. Phys.* **1996**, *79*, 2136. (b) Brown, A. R.; Pomp, A.; Hart, C. M.; de Leeuw, D. M. *Science* **1995**, *270*, 972.

(8) Dimitrakopoulos, C. D.; Brown, A. R.; Pomp, A. *J. Appl. Phys.* **1996**, *80*, 2501.

(9) Lin, Y. Y.; Gundlach, D. J.; Jackson, T. N. *54Th Annual Device Research Conference Digest* **1996**, 80. See also: *Science* **1996**, *273*, 879.

(10) Minakata, T.; Imai, H.; Ozaki, M.; Saco, K. *J. Appl. Phys.* **1992**, *72*, 5220.

(11) Dodabalapur, A.; Torsi, L.; Katz, H. E. *Science* **1995**, *268*, 270−271.

(12) Sze, S. M. *Physics of Semiconductor Devices*; Wiley: New York, 1981.

(13) Warta, W.; Stehle, R.; Karl, N. *Appl. Phys.* **1985**, *A36*, 163.

S0897-4756(96)00366-3 CCC: $12.00

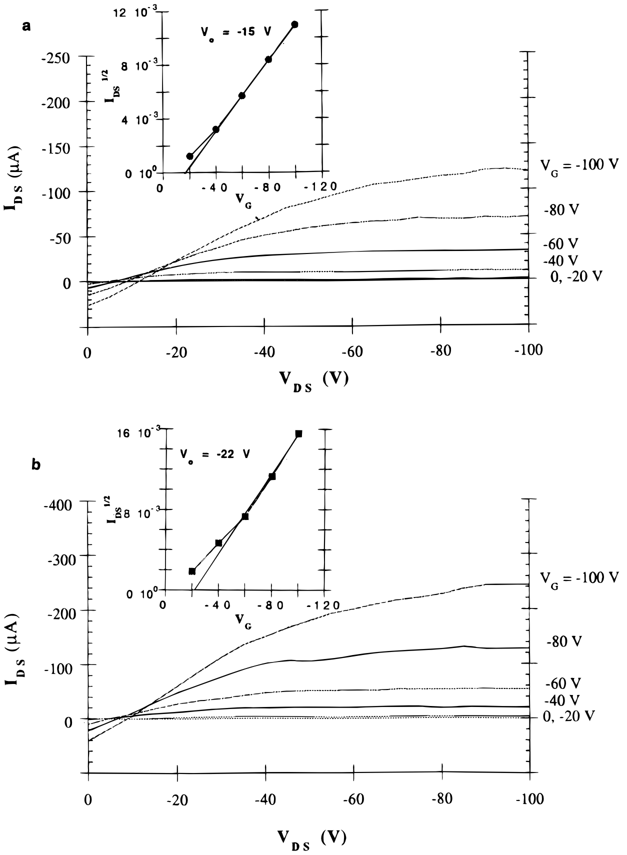

Figure 1. Source-drain current vs voltage (I_{DS} vs V_{DS}) characteristics of pentacene TFTs with $L = 12\ \mu$m at different gate voltages deposited at (a) $T_{sub} = 25$ °C (inset, plot of I_{DS} $^1/_2$ vs V_{GS} to calculate the extrapolated threshold voltage, $V_0 = -15$ V) and (b) $T_{sub} = 85$ °C (inset, plot of I_{DS} $^1/_2$ vs V_{GS} to calculate the extrapolated threshold voltage, $V_0 = -22$ V).

measured at a certain V_{DS} in the saturation regime, of 10^3-10^5 were achieved.

X-ray diffraction studies show that pentacene films deposited at all T_{sub} on Si/SiO$_2$ in the same process as for device fabrication are highly ordered with a sharp reflection at 2θ of 5.9° (d = 14.97 Å). This peak can be indexed as the 001 reflection corresponding to the crystallographic repeat along the molecular chain, similar to that reported by Minakata et al.[10] This observation combined with the absence of corresponding 00*l* reflections in the electron diffraction pattern at normal beam incidence implies that the pentacene molecules stand with their long axes essentially perpendicular to the substrate. Thus, the direction of high mobility is parallel to substrate and perpendicular to the long axis of the pentacene molecule. The same molecular orientation was observed for α-6T and was deemed very beneficial for device optimization since the high mobility direction is along the direction of the carrier transport in the transistor.[14]

Figure 2a,b shows the morphologies of the films deposited at substrate temperatures, T_{sub} = 25 and 85 °C, respectively. As seen from the micrographs, both films appear to consist of irregular grains whose average sizes (about 400 nm) are almost identical. However, there is a very strong temperature dependence of pentacene nucleation and growth, which can lead to formation of much larger underlying single-crystalline domains having extensive crystallographic coherence. This can be seen in the electron-diffraction patterns in Figure 3a,b. At T_{sub} = 85 °C, the very sharp and narrow diffraction spots indicate the formation of large single-crystal domains as compared to the case at T_{sub} = 25 °C, where there is only a hint of structural correlations among the grains. The exact areas from which the diffraction patterns originated in each case are delineated by a superposed double exposure showing the selector aperture inserted at the intermediate image plane of the electron microscope. This demonstrates that over areas 3 μm in diameter (i.e., the diameter of the diffraction aperture) there is a common single-crystal orientation among the hundreds of grains contained therein. Use of a larger selector aperture (up to 10 μm diameter) gave similar results with only slight arcing of the reflections, indicating small mutual misorientations among the crystals. Such long-range interconnected and space-filling single-crystal-type morphologies are exceedingly rarely attainable by direct evaporation. In the cases of other organic materials such as α-6T[5,15] and Cu−phthalocyanine,[16] which form p-type TFTs, grain sizes increase with increasing substrate temperature or rapid thermal annealing but do

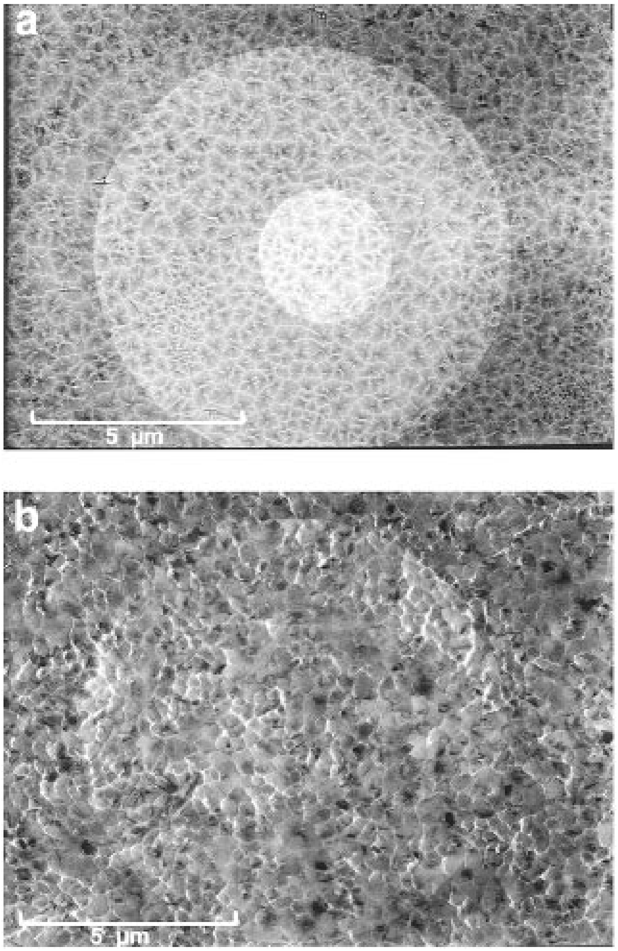

Figure 2. Transmission electron micrographs from pentacene films (thickness ca. 500 Å) deposited at (a) T_{sub} = 25 °C and (b) T_{sub} = 85 °C.

---

[14] Garnier, F.; Yassar, A.; Hajlaoui, R.; Horowitz, G.; Deloffre, F.; Servet, B.; Ries, S.; Alnot, P. *J. Am. Chem. Soc.* **1993**, *115*, 8716.

[15] Torsi, L.; Dodabalapur, A.; Lovinger, A. J.; Katz, H. E.; Ruel, R.; Davis, D. D.; Baldwin, K. W. *Chem. Mater.* **1995**, *7*, 2247.

[16] Bao, Z.; Lovinger, A.; Dodabalapur, A. *Appl. Phys. Lett.*, in press.

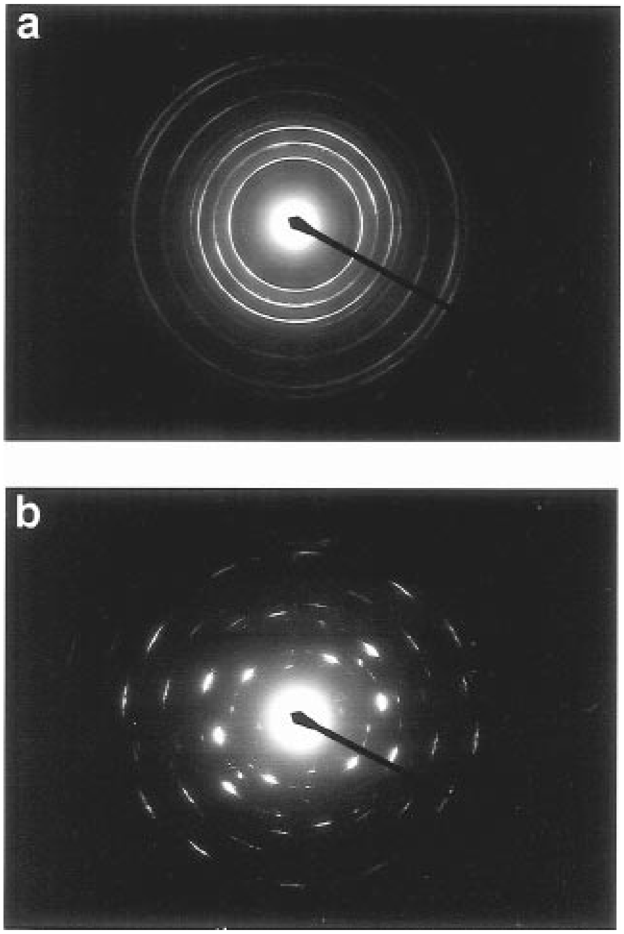

Figure 3. Selected-area electron diffraction patterns of pentacene films (thickness ca. 500 Å) deposited at (a) $T_{sub} = 25$ °C and (b) $T_{sub} = 85$ °C using 3 μm diffraction aperture diameter.

not coalesce into a common single-crystalline orientation.

Similar TFT and morphological characterizations were done for films deposited at 55 °C. Calculated mobilities were similar to that obtained for films deposited at 25 °C, although the electron diffraction pattern was closer to the $T_{sub} = 85$ °C case. However, the number of devices that functioned reliably for TFTs deposited at 55 °C was higher (ca. 90% of the devices tested) than for the two other temperatures (less than 25%). This leads us to believe that the relatively lower mobility and lesser number of working devices at room temperature is possibly due to the poorer connections and increased misorientations among crystals. While single-crystal domains are formed at 85 °C, which translates to a higher mobility in this case, the yield of working devices was generally lower, possibly due to shrinkage-induced delamination from the contacts.

We believe that the formation of large single-crystal domains in vacuum-deposited pentacene TFTs and the high degree of molecular ordering that this implies are correlated with the high mobilities obtained from these devices. In previous work, such high mobilities could have been attributed to top-contact geometry because of the possibly more facile charge injection from top contacts.[9] It may well be that the yield of working devices is improved using the top contact fabrication schemes. The extended single-crystal nature of the pentacene films could lead to severely diminished mobilities where crystal domain boundaries occur, which can lead to nonworking devices. However, our results do demonstrate that the high mobility is intrinsic to the pentacene in the present morphology, and can in fact be obtained with bottom contacts.

Acknowledgment. The authors would like to thank Z. Bao, E. Reichmanis, and R. Slusher for stimulating discussions. We are also grateful to T. Jackson and C. Dimitrakopoulos for sharing their results prior to publication.

CM9603664